Supporting Information

Salt-Mediated, Plasmonic Field-Field/ Field-Lattice Couplings-Enhanced NIR-II Photodynamic Therapy using Core-gap-shell Gold Nanopeanuts

*Naresh Kuthala[1], Munusamy Shanmugam[1], Xiangyi Kong[3], Chi-Shiun Chiang[2], Kuo Chu Hwang[1]**

[*]Prof. Kuo Chu Hwang, Naresh Kuthala, Munusamy Shanmugam,
1. Department of Chemistry,
National Tsing Hua University, Hsinchu 30013, Taiwan ROC.
E-mail: kchwang@mx.nthu.edu.tw

Prof. Chi-Shiun Chiang,
2. Department of Biomedical Engineering and Environmental Sciences,
National Tsing Hua University, Hsinchu 30013, Taiwan ROC.

Dr. Xiangyi Kong,
3. Department of Breast Surgical Oncology, National Cancer Center/National Clinical Research Center for Cancer/Cancer Hospital, Chinese Academy of Medical Sciences and Peking Union Medical College, Beijing, 100021, China.

Experimental Section

Synthesis of Au nanorods (aspect ratio ~4.0): Au NRs were synthesized via a seed-mediated growth method with slight modification. Briefly, in the seed preparation, 5 mL of 0.2 M CTAB aqueous solution was mixed with 5 mL of $HAuCl_4{\cdot}3H_2O$ (0.5 mM), followed by addition of 0.6 mL of freshly prepared ice cold 0.01 M $NaBH_4$ (diluted to 1 mL) under vigorous stirring until the color changes from yellow to brownish yellow. Further the seed solution was preserved at room temperature for 30 min. In the growth solution, 9 g of CTAB and 1.234 g sodium oleate were dissolved in 250 mL DI water at 50 °C, and then the solution temperature was maintained at 30 °C. Then, 18 mL of 4 mM $AgNO_3$ was added without any disturbance for 15 min at 30 °C. After that, 250 mL of 1 mM $HAuCl_4.3H_2O$ was added with vigorous stirring at 700 rpm for 90 min, followed by addition of concentrated HCl (1.5 mL) with 400 rpm for 15 min. Then, a mild reducing agent ascorbic acid (1.25 mL, 0.064 M) was added with vigorous stirring for 30 sec. Finally, 0.2 mL of seed solution was added with vigorous stirring of 30 sec and aged for 12 h at 30 °C. Then, as-synthesized Au NRs were used for the subsequent synthesis of Au-Ag core shell NRs.

Synthesis of Au@Ag core-shell NRs*:* Briefly, 1 mL of Au NRs (50 ppm) solution was centrifugated. Au NRs were collected, and re-suspended in an aqueous solution containing 1 mL (50 mM) CTAB as well as 5 mL of 1 wt % poly(vinylpyrrolidone) (PVP, M_W= 55,000). Then, a certain volume (V= 500 µL for an Ag shell of 7-8 nm thickness, and V= 1000 µL for an Ag shell of 9-10 nm) of 1 mM of $AgNO_3$ was added for generation of a thin Ag shell. Then, 0.125 mL of ascorbic acid (100 mM) and 0.25 mL of NaOH (0.1 M) were added

sequentially with stirring for 10 min. The as-formed green Au@Ag core-shell NRs were collected by centrifugation at 9,000 rpm for 8 min, and washed with DI water twice.

***Synthesis of Au NPNs**:* Au NPNs were synthesized via a galvanic replacement reaction of the Ag shell in the Au NR@Ag core-shell nanorods by $HAuCl_4.3H_2O$. In brief, 550 µL of 0.94 mM Au NR@Ag core-shell NRs were dispersed in 5.75 mL DI water, then sequentially added 500 µL of 100 mM CTAB, and 125 µL of 100 mM ascorbic acid with slow stirring at 400 rpm. Different volumes (V= 700 µL for 2.0 nm gap and V= 400 µL for 6.5 nm gap) of 1 mM $HAuCl_4.3H_2O$ were added with continuous stirring for 16 min to complete the reaction. Then the reaction contents were centrifuged at 6000 rpm for 10 min, collected, and washed with DI water, and re-dispersed in DI water.

***Synthesis of Au NPNs with tunable LSPR in the broad NIR region**:* As-synthesized Au NPNs 2.0 and 6.5 were treated with 1.67 M $NaCl_{(aq)}$ aqueous solution under slow stirring at room temperature for overnight. Then, the contents were washed with DI water and re-dispersed in DI water for further characterization.

Further, the effect of NaCl on the UV-vis-NIR broad absorption of Au NPNs6.5 was evaluated sequentially using different NaCl concentrations of 0, 0.5, 1, 1.67, 2, and 5 M, respectively. Likewise, the effects of other salts, such as NaBr, NaI, $MgSO_4$, $MgCl_2$, and $(NH_4)_2SO_4$ on the UV-vis-NIR broad absorption of Au NPNs6.5 were investigated in a similar way.

***Stability of Au NPN6.5(NaCl) in a NaCl (0.125 M) aqueous solution**:* As synthesized Au NPN6.5(NaCl)(1.67 M) after multiple washings were dispersed in a physiological aqueous solution containing 0.125 M NaCl under constant slow stirring at room temperature. And the UV-vis-NIR spectra were recorded at time points 0, 12, 24, 48, and 72 h, respectively.

***Surface modification of Au NPNs**:* Finally, 5 mL of stock Au NPNs were diluted to 10 mL and then conjugates with 11-MUA (Mercapto Undecanoic Acid, 100 µL of 0.01 M) under constant stirring for 4 h at room temperature. After multiple washes, 12.8 µmol EDC and 13 µmol NHS were added to the Au NPNs-S-COOH aqueous solution with 10 min incubation, followed by addition of 40 µL of anti-h-EGFR (R&D systems, Minneapolis, USA) under constant stirring for 4 h at ice cold temperature. Further, the Au NPNs-S-E was washed and stored at 4 °C for bio-imaging and PDT/PTT therapeutic applications. For the imaging purposes, the Au NPN6.5(NaCl) was modified with anti-EGFR and cy5.5 via EDC coupling. The LSPR properties of Au NPNs 2.0 and 6.5 nm gaps were monitored using UV-Vis-NIR spectrometer (Model: JASCO V-540). The elemental analysis of Au and Ag was evaluated by EDAX mapping and transmission electron microscopy images in a JEM-2100 (JEOL Ltd, Tokyo, Japan) electron microscopy with an operation voltage of 200 kV.

Singlet oxygen phosphorescence measurements: Au NPNs 2.0 and 6.5 nm (1 mg/mL) were dispersed in D_2O to monitor phosphorescence emission of singlet oxygen upon NIR light excitation. Singlet oxygen phosphorescence was recorded using luminescence spectrometer (FLS920, Edinburgh, equipped with a 450 W broadband Xe lamp). Scattering light and stray light shorter than 1100 nm were filtered by an 1100 nm long pass filter (Newport, LP1100) located in-between the sample and the detector.

EPR measurements: For the detection of hydroxyl radical (·OH), anti-EGFR-Au NPN 6.5 NaCl (1 mg/mL) were dispersed in water. In a typical experiment, 1.0 M 5,5-dimethyl-1-pyrroline N-oxide (DMPO) was mixed with anti-EGFR-Au NPN 6.5 NaCl. The resulting solution mixture was then irradiated with 808 and 1064 nm lasers, respectively, at a power intensity of 200 mW/cm^2 for 5 min under constant stirring. The solution was then monitored using EPR. For hydroxyl radical quenching experiments, 10 mM Mannitol was used as a ·OH scavenger.

For the singlet oxygen ($^1O_2$) detection using EPR, anti-EGFR-Au NPN 6.5(NaCl) (1 mg/mL) were dispersed in D_2O. In a typical experiment, 1.0 M, 2,2,6,6-tetramethylpiperidine (TEMP) probe in D_2O solution was mixed with anti-EGFR-Au NPN 6.5(NaCl). The resulting solution mixture was then irradiated with 808 nm, and 1064 nm lasers at a power intensity of 200 mW/cm^2 for 5 min under constant stirring. The solution was then monitored using EPR. For singlet oxygen quenching experiments, 10 mM sodium azide was used as a $^1O_2$-specific scavenger.

Calculation of molar extinction coefficients of Au NPNs: To determine the molar extinction coefficients of Au NPNs, firstly, the average size of the nanomaterial has to be determined by TEM images (n= 20). By knowing the average size (and thus estimated volume of a nanoparticle), the density of the Au metal, and atomic weight, one can calculate the number of Au atoms per nanoparticle. Secondly, the total concentration of gold atoms in a solution was determined by ICP-MS measurements. Thirdly, Dividing the total concentration of gold atoms in a solution by the number of gold atoms in a nanoparticle, one can obtain the number (and thus the concentration) of nanoparticles in the solution. Fourthly, the extinction coefficients (ε) of a nanoparticle, here Au NPNs, could be obtained from the Beer's law, ε = A/bc, where b = 1 cm, and c = concentration of Au NPNs.

Cell culture: The murine colorectal carcinoma cell line CT26.WT (ATCC® CRL-2638™) was obtained from ATCC (American type culture collection). The cell culture conditions were maintained according to the standard protocols provided by ATCC. The complete growth medium is RPMI-1640 with sodium pyruvate (1 mM), L-glutamine (2 mM), and sodium bicarbonate (1500 mg/L) with final addition of penicillin streptomycin (1%) and fetal bovine serum (10%). In vitro experiments were carried out in an incubator supplied with 5% CO_2 (95 % humidity) and the temperature maintained at 37 °C.

Cytotoxicity evaluation*:* The cytotoxicities of AuNPN6.5 and AuNPN6.5(NaCl) towards the CT-26 WT cancer cell line were measured using the MTT (3-(4,5-dimethylthiazol-2-yl)-2,5-diphenyltetrazolium bromide) assay. The CT26.WT cancer cells with a density of 2 x 10^4 cells/mL was loaded into a 96 well plate and incubated at 37 ˚C for 24 h. Then, different amounts of 0, 10, 25, and 50 μg/mL of nanoparticles were added to the cells, and incubated for another 24 h. Then, the cells were photo irradiated with 808 (200 mW/cm^2, 10 min), or 1064 nm (200 mW/cm^2, 11 min), respectively. The irradiation time at different wavelengths were adjusted according to the extinction coefficients of Au NPN6.5 (or Au NPN6.5(NaCl)) at 808 and 1064 nm, so that the amounts of photons being absorbed by a nanomaterial are the same at these two wavelengths. Then the cell viabilities were evaluated by the standard protocols of MTT assay.

Cellular uptake evaluation - CLSM*:* The CT-26.WT cells with a density of 2 x 10^4 cells/mL was loaded into the 6 well plate with glass cover slip, and incubated at 37 °C for 24 h. Further, the cells were incubated with different amounts of Au NPN6.5(NaCl)-Cy5.5 for 12 h at 37 °C. Finally, the cells were washed with 1x PBS, and fixed with 4% p-HCHO, then tween-20, and finally addition of DAPI to stain the nucleus. The cells were analyzed under CLSM for fluorescence imaging.

In vitro uptake of anti-EGFR-*Au NPN6.5 *by CT-26 WT cells: CT-26 WT cells (2 x 10^5 cells / mL) were cultured in a 6-well plate and incubated for 24 h. Then, the cells were incubated with different concentrations of anti-EGFR-Au NPN6.5(NaCl) and Au NPN6.5(NaCl), followed by incubation for another 24 h. In the next day, the cells were washed with 1× PBS, followed by trypsinization. The cells were then stained with Cy5®goat anti mouse IgG secondary antibody (Lot No. 1675775, Life technologies corporation, USA) with 5 µg/mL per flow tube and incubated for 1 h at 4 °C. The cells were then washed thoroughly to remove any unbound secondary antibody, put in 1 mL of 1× PBS, and subjected to flow cytometric analysis. The fluorescence from APC-A (λ_{ex} = 650 nm; λ_{em} = 667 nm) was detected from the flow cytometer.

For the detection of fluorescence using confocal optical microscopy, the same number of CT-26 WT cells were loaded. After incubating overnight, the cells were loaded with different concentrations of anti-EGFR-Au NPN6.5(NaCl) and Au NPN6.5(NaCl), and then incubated for 24 h, followed by washing with 1× PBS and fixation using 4% paraformaldehyde in PBS for 10 min. The cells were then stained with Cy5®goat anti mouse IgG secondary antibody (Lot No. 1675775, Life technologies corporation, USA) with 5 µg/mL per well, and incubated for 1 h at 4 °C. Finally, the cells were washed with 1× PBS and the nucleus were stained with DAPI (4',6-diamidino-2-phenylindole). The samples were then examined under a confocal laser scanning microscopy (LSM 700, Zeiss) equipped with 405 nm and 655 nm lasers. The fluorescence emission was monitored for DAPI (λ_{em}= 460 nm) and Cy5 (λ_{em} = 667 nm) channels, respectively.

Calcein AM or PI staining: CT-26 WT cancer cells with a density of 2 x 10^4 cells/mL was loaded into a 6-well plate with glass cover slip, and incubated at 37 ˚C for 24 h. Further, the cancer cells were incubated with different amounts of Au NPN6.5 and Au NPN6.5(NaCl) for 12 h at 37 °C. Then, old medium was removed, and cells were washed with 1x PBS. After photo-irradiation with 808, or 1064 nm laser, respectively, the cells were incubated with 10 µg/mL of Calcein AM and 50 µg/mL of PI for 20 min. Then, the cells were washed and fixed for the confocal optical microscopy analysis.

DCFH-DA and SOSG probes for confocal imaging: CT26.WT cells (2 x 10^5 cells/mL) were loaded into a 6-well dish and incubated for 24 h. Then, the cells were fed with different amounts of Au NPN6.5 and Au NPN6.5(NaCl), and further incubated for 12 h. To detect ROS ($^1O_2$), the cells were incubated with 2,7-dichlorofluorescien diacetate (DCFH-DA) or singlet oxygen sensor green (SOSG) solution (5 µM in cell culture medium) for 30 min at 37 °C. After photo-irradiation with 808, or 1064 nm laser, respectively, the cells were workup and examined in the FITC channel by confocal optical microscope.

ROS-in vitro detection: CT26.WT cells (2 x 10^5 cells/mL) were loaded into a 12-well dish and incubated for 24 h. Further, the cells were fed with different amounts of Au NPN6.5 and Au NPN6.5(NaCl), and further incubated for 12 h. To detect ROS, the cells were incubated with 2,7-dichlorofluorescien diacetate (DCFH-DA) solution (5 μM in cell culture medium) for 30 min at 37 ^oC. After photo-irradiation with 808, or1064 nm laser, respectively, the cells were workup and examined in the FITC channel in flow cell cytometry. Additional quenching experiments were carried out by incubating the cells with 50 mM NaN_3 (in PBS) for 1 h, and the rest of process is the same as the above protocol.

Heat shock protein in vitro analysis: CT26.WT cells (2 x 10^5 cells/mL) were loaded to a 12-well dish, and incubated for 24 h. Further, the cells were fed with different amounts of Au NPN6.5 and Au NPN6.5(NaCl), and further incubated for 12 h. After photo-irradiation with 808, or 1064 nm laser, FITC conjugated HSP-70 antibody (1:50 dilution; Cell signaling, USA) was added into the solution immediately. The cells were then workup, and examined in the FITC channel by flow cell cytometry.

IVIS imaging and in vivo PDT and PTT experiments: CT26.WT cells (2 x 10^6 cells/mL) in a PBS-containing solution were injected into the right leg muscle of female BALB/C nude mice. After tumors reach 3-4 mm in diameter, the mice were classified randomly into 8 groups, and injected with anti-h-EGFR-Au NPN6.5(NaCl)-Cy5.5 intravenously. After 24 h of i.v. injection, the mice were monitored under the Xenogen IVIS imaging system under the cy5.5 channel selection. The mice were photo-irradiated with 808 nm laser (200 mW/cm^2, 10 min) or 1064 nm laser (200 mW/cm^2, 11 min) once every other day (i.e., once every two days) with iv injection of NPs twice at day 0^{th} and day 7^{th}. The laser power and irradiation time at different wavelengths were adjusted so that the numbers of photons being absorbed by nanomaterials are the same, which allows comparison of phototherapy effects of different wavelengths. We check the extinction coefficients at 808 nm and 1064 nm. We have fixed the time of 808 nm (10 min) and calculated the time for 1064 nm with respect to extinction coefficients (11 min) with identical power densities of 200 mW/cm^2 for both wavelengths. The control group was monitored without photo-irradiation. Doxorubicin (a well-known clinical anti-cancer drug), PBS and anti-h-EGFR-Au NPN6.5 and anti-h-EGFR-Au NPN6.5(NaCl) (50 mg/kg) were injected through tail vein (single time). Survival rate, body weights and tumor growths were monitored throughout the therapy every day. All the animal experiments were approved by the Institutional Animal Care & Utilization Committee, National Tsing Hua University (IACUC No. 109052).

Tumor volume calculation: Tumor volume was estimated by using the following equation: tumor volume= (π x length x width^2)/ 6, where length is the largest tumor diameter (in mm) and width is the tumor diameter (in mm) in the perpendicular direction (ref. Lab. Animal 2013, 42, 217-224)..

Histology analysis: At the end of therapy, tumor tissues, and major organs, including liver and spleen, were collected. Each organ was cut into 10 μm thickness per slice. To analyze the damages at different organs before and after PDT/PTT, the slices were stained with H&E (hematoxylin and eosin) and gone through microscopic examination.

Caspase-3 staining: Caspase-3 staining was used to determine the extent of apoptosis in the tumor tissues. At the end of therapy, tumor tissues, and major organs, including liver and spleen, were collected. Each organ was fixed with PFA (Paraformaldehyde)/Formalin, then embedded into paraffin. Each organ was cut into 10 μm thickness per slice and deparaffinized in xylene and ethyl alcohol. Then, each section was incubated in 3% goat serum for 2 h, followed by incubation with caspase-3 (1:20) (ab2302) primary antibody. After washing, sections were further incubated with a secondary antibody for 1 hour. After washing steps, the staining was examined using fluorescence microscope.

In vivo thermal imaging: Anti-h-EGFR-Au NPN6.5 and anti-h-EGFR-Au NPN6.5(NaCl) (50 mg/Kg) and PBS were injected intravenously into CT26.WT cancer cells-implanted BALB/C nude mice. After 24 h, the tumor regions were irradiated with 808, or 1064 nm CW lasers. The temperature at the tumor regions were measured precisely every minute by NIR thermal camera (Thermo shot F30). The image data was processed by TAS 19 software.

In vivo toxicity assay of anti-EGFR-Au NPNs6.5(NaCl): Targeted Au NPN6.5, Au NPN6.5(NaCl) (50 mg/Kg), and PBS were injected intravenously in CT26.WT cells-implanted BALB/C nude mice. After 45 days, the blood serum samples were collected for the analysis of standard pathological assays to examine the lever and nephritic functions.

Statistics: The statistics data analyzed using two-way ANOVA test function provided by the GraphPad Prism 5 software. Kaplan-Meier method was used for survival curve plots. The statistical significance of all figures was denoted by $*p < 0.05$; $**p < 0.01$; $***p < 0.001$.

Photothermal conversion efficiencies: To estimate the photothermal efficiencies of AuNPN6.5/ AuNPN6.5(NaCl), we followed the reported protocols. The photothermal photothermal efficiencies of Au NPN6.5 /Au NPN6.5(NaCl), under 808 or 1064 nm (both 200 mW/cm^2) CW laser irradiation, were calculated by the following equations. Au NPN6.5/ Au NPN6.5(NaCl) aqueous solutions were irradiated with 808 nm for 10 min to reach the steady state temperature. After turning off the laser, the decrease in the temperature of the aqueous solution was noted to measure Au NPN6.5/ Au NPN6.5(NaCl) heat transfer rate to surroundings. The expression for photothermal conversion efficiency, η, at 808 nm can be calculated as below.

$$\eta = hS\,(T_{max} - T_{surr}) - Q_{dis} / I(1\text{-}10^{-A_{808}}) \text{-}\ldots\ldots\ldots\ldots\ldots (1)$$

In case of Au NPN6.5(NaCl), the laser power (I) is 200 mW/cm^2, the absorbance of at 808 nm is 1. T_{surr} represents the surrounding temperature which is 30 ^oC, the maximum temperature T_{max} is 43.1 ^oC (obtained from Figure S12 (c)). Hence, the value of $T_{max} - T_{surr}$ is 13.1 ^oC. Then, the hS value was estimated from Figure S12 (d), where S represents the surface area and h the heat transfer coefficient. From the expression,

$$\theta = T - T_{surr} / T_{max} - T_{surr} \text{-}\ldots\ldots\ldots\ldots\ldots\ldots\ldots\ldots (2)$$

We can evaluate the value of hS using the above equation. From equation (3), the time constant was calculated

$$t = -\zeta_s \ln(\theta) - \ldots\ldots (3)$$

Finally, $$hS = m_{D\,x}\, c_D / \zeta_s - \ldots\ldots (4)$$

$$hS = 0.25 \times 4.2 / 271.9 \text{ J/sec } ^oC = 3.86 \text{ mW/ } ^oC$$

$$Q_{dis} = m \times C \times \Delta T = 0.25 \times 6.9 \times 2 = 3.45 \text{ mW.}$$

η value can be obtained by substituting all values into the equation (1),

$$\eta = 3.86 \times (14) - 3.45 / 200\,(1-10^{-1}) = 28.1\ \%$$

PTT efficiency of Au NPN6.5(NaCl) at 808 nm is 28.1%, i.e., η = 28.1 %

The photothermal conversion efficiency of Au NPN6.5(NaCl) at 1064 nm can be calculated in a similar way. The laser power, I, is 200 mW/cm^2, the absorbance of Au NPN6.5(NaCl) at 1064 nm is 0.94. $T_{max} - T_{surr}$ is 5.2 ^{o}C.

$$hS = 0.25 \times 4.2 / 190.5 \text{ J/sec } ^oC = 5.5 \text{ mW/ } ^oC$$

$$Q_{dis} = m \times C \times \Delta T = 0.25 \times 6.34 \times 1.1 = 1.74 \text{ mW.}$$

η value can be obtained by substituting all values in the equation (1),

$$\eta = 5.5 \times (5.2) - 1.74 / 200(1-10^{-0.94}) = 15.1\ \%$$

PTT efficiency of Au NPN6.5(NaCl) at 1064 nm is η = 15.1 %

The photothermal conversion efficiency of Au NPN6.5 at 808 nm can be calculated in a similar way. The laser power, I, is 200 mW/cm^2, the absorbance of Au NPN6.5 at 808 nm is 0.94. $T_{max} - T_{surr}$ is equal to 3 ^{o}C

$$hS = 0.25 \times 4.2 / 211.4 \text{ J/sec } ^oC = 4.96 \text{ mW/ } ^oC$$

$$Q_{dis} = m \times C \times \Delta T = 0.25 \times 6.9 \times 2 = 3.45 \text{ mW.}$$

η value can be obtained by substituting all values in the equation (1),

$$\eta = 4.96 \times (3) - 3.45 / 200(1-10^{-0.94}) = 6.4\ \%$$

PTT efficiency of Au NPN6.5 at 808 nm is 6.4%, i.e., η = 6.4 %

The photothermal conversion efficiency of Au NPN6.5 at 1064 nm can be calculated in a similar way. The power of laser (I) is 200 mW/cm^2, the absorbance of Au NPN6.5 at 1064 nm is 0.33. $T_{max} - T_{surr}$ is 2 ^{o}C.

$$hS = 0.25 \times 4.2 / 293.7 \text{ J/sec } ^oC = 3.57 \text{ mW/ } ^oC$$

$$Q_{dis} = m \times C \times \Delta T = 0.25 \times 6.34 \times 1.1 = 1.74 \text{ mW}$$

η value can be obtained by substituting all values in the equation (1),

$$\eta = 3.57 \times (2) - 1.74 / 200(1-10^{-0.33}) = 5\ \%$$

PTT efficiency of Au NPN6.5 at 1064 nm is η = 5 %

Singlet O_2 phosphorescence Quantum yield measurements using samples with OD= 0.1: We have used a quartz cuvette with a path length of 1 cm and 1 mL capacity in the experiments. The concentrations of Au NPNs and the methylene blue reference standard dye were adjusted to have a OD value of 0.1 at their excitation wavelengths (650 nm for methylene blue and 1064 nm for Au NPNs), respectively, to mininize the scattering and inner filter effects from the reference dye and the naomaterials. To determine the quantum yield of singlet O_2 formed via sensitization by Au NPNs6.5(NaCl) upon 1064 nm NIR light excitation, we use methylene blue as a reference standard, and measure the singlet O_2 formation yield of Au NPN6.5(NaCl) by comparing the phosphorescence emission area of singlet O_2 (integration area from 1225 to 1300 nm) with that obtained using methylene blue as a photo-sensitizer. The singlet O_2 phosphorescence emission spectra from Au NPN6.5(NaCl) and methylene blue were shown in the Figure 2d in the main text, whereas those for Au NPN6.5 and methylene blue were shown in the Figure S5. Phosphorescence emission area, $Area_{phos,MB}$ is equal to the multiplication product between the absorbance of methylene blue at 650 nm (Ab_{MB-650}), incident light intensity at 650 nm (2 mW/cm^2, slit width: 10 nm) from the luminescence spectrometer, and the singlet O_2 formation yield (Φ_{MB}), i.e., the equation (1). The singlet O_2 generation quantum yield of MB in D_2O is known to be 0.68.

$$Area_{phos\text{-}MB} = Ab_{MB\text{-}650} \times I_{650} \times \Phi_{MB} \quad \ldots\ldots\ldots\ldots (1)$$

$Area_{phos\text{-}MB} = 144357658$

Similar equation can be derived for Au NPN6.5(NaCl) (see equation (2))

$$Area_{phos\text{-}AuNPN6.5(NaCl)\text{-}1064\ nm} = Ab_{AuNPN6.5(NaCl)\text{-}1064\ nm} \times I_{1064} \times \Phi_{AuNPN6.5(NaCl)\text{-}1064\ nm} \quad \ldots\ldots\ldots\ldots(2)$$

$Area_{phos\text{-}AuNPN6.5\ (NaCl)\text{-}1064nm} = 156096858$

The incident light intensity of FLS 920 spectrometer at 1064 nm (~8.3 mW/cm^2, slit width: 10 nm). The absorbances of both methylene blue and Au NPN6.5(NaCl) solution at their excitation wavelengths were adjusted to 0.1. After substituting all the parameters and dividing equations (1)/ (2), one can obtain the value of $\Phi_{AuNPN6.5(NaCl)\text{-}1064\ nm}$ to be 0.35 @1064 nm.

Similarly, the singlet O_2 quantum yields of Au NPN6.5 (without filling $NaCl_{(aq)}$ in the nanogaps) at 1064 nm was measured and calculated in the similar manner using the values of $Area_{phos\text{-}AuRS6.5\text{-}1064} = 78592719$. The final singlet O_2 quantum yield for $\Phi_{AuNPN6.5\text{-}1064\ nm}$ was determined to be 0.17 @1064 nm.

In the singlet oxygen quantum yield measurements, it is better to have the same excitation wavelength for both the reference standard dye and the system to be measured in the singlet oxygen quantum yield measurement. When the same excitation wavelength was used for both the reference standard dye and the nanomterial/molecule to be measured, all solvent factors and instrument factors are the same and cancelled out. Therefore, it is not necessary to consider both the solvent factors and instrument factors in the calculation of singlet oxygen quantum yield. However, this requirement is not absolutely necessary. In the literature, it was also reported that phenalenone dye was used as the reference standard dye using 365 nm for excitation in the singlet oxygen quantum yield measurement for an acridinium derivative

of IR-1061 acridinium dye using 1064 nm for excitation (see, ***Chem. Commun.,*** 2019, 55, 5511). To date, there is lack of reference standard dye in the NIR region for singlet oxygen quantum yield measurements of a new photosensitizer. Therefore, a reference standard dye, such as methylene blue, with different excitation wavelength must be used. When the excitation wavelength for the quantum yield reference standard is different from the wavelength used for excitation of our Au NPNs, some possible deviations may occur and lead to inaccurate quantum yield for a system to be measured. These possible deviations include (a) the difference in the solvent absorbance, here H_2O/D_2O in our system, at the two excitation wavelengths, i.e, 650 nm (for methylene blue) and 1064 nm (for our Au NPNs), and (b) the difference in the excitation light intensities at 650 nm and 1064 nm in the phosphorescence spectrometer. As long as these possible deviations were corrected in the calculation, a nearly accurate singlet oxygen generation quantum yield still can be obtained. In the current system, D_2O was used as the solvent for dissolution of methylene blue (the reference standard with known singlet oxygen generation quantum yield of 0.68) and H_2O for our anti-h-EGFR-Au NPN6.5(NaCl). The absorbances of D_2O/H_2O at 650 nm and 1064 nm are negligibly small as compared to the OD values of 0.1 or 0.2 for methylene blue and the anti-h-EGFR-Au NPN6.5(NaCl). In addition, the absorption spectrum of H_2O/D_2O was used as the background in our UV-visible-NIR absorption measurements. Therefore, the difference in the absorbance of D_2O/H_2O at 650 nm and 1064 nm were subtracted from the OD measurements for both methylene blue and the anti-h-EGFR-Au NPN6.5(NaCl). In other words, the difference in the absorbance of D_2O/H_2O at 650 and 1064 nm does not contribute in our calculation for the singlet oxygen generation quantum yield. For the possible deviation (b), the excitation light intensities at 650 nm and 1064 nm need to be measured and calibrated in the calculation of singlet O2 QY calculation (i.e., the above equations (1) and (2)). Therefore, the instrument factor about the difference in the excitation light intensities at 650 nm and 1064 nm used in the singlet O2 phosphorescence intensities has to be calibrated in the above calculation of singlet oxygen quantum yields.

To calibrate the inner filter effects from (i.e., the absorption of singlet O_2 phosphorescence emission light by) Au NPNs on the singlet O_2 phosphorescence intensty detected within 1200-1300 nm range, the following equation for absorbance was used.

$$\text{Absorbance} = -\log(I/I_0)$$

By substitutimg the absorbance of anti-h-EGFR-Au NPN6.5(NaCl) with an OD value of 0.079 and anti-h-EGFR-Au NPN6.5 with an OD value of 0.06 at 1260 nm in the above equation yields 83.3% transmission of singlet O_2 phosphorescence light through the solution in the case of anti-h-EGFR-Au NPN6.5(NaCl) and 87% transmission of singlet O_2 phosphorescence light though the solution in the case of anti-h-EGFR-Au NPN6.5. Hence the true singlet O_2 generation qunamtum yields for $\Phi_{\text{AuNPN6.5(NaCl)+1064 nm}}$ to be (0.35/0.833=) 0.42@1064 nm and $\Phi_{\text{AuNPN6.5+1064 nm}}$ to be (0.17/0.87=) 0.20@1064 nm, respectively..

Singlet O_2 phosphorescence Quantum yield measurements using samples with OD= 0.2: Similar to the above singlet O_2 phosphorescence QY measurements using Au NPNs samples

with OD= 0.1, we repeated the experiments using Au NPNs samples with OD= 0.2 (at 1064 nm). The singlet O_2 phosphorescence emission spectra from methylene blue (λ_{ex}= 650 nm, OD= 0.2 in D2O), and Au NPN6.5 (in H2O solution with OD= 0.2 at 1064 nm) and Au NPN6.5(NaCl) (in 1.67 M NaCl-H_2O solution, OD= 0.2 at 1064 nm) were shown below. Similarly, methylene blue was used as a reference standard, to measure the singlet O_2 formation yield of Au NPN6.5(NaCl) by comparing the phosphorescence emission area of singlet O_2 (integration area from 1225 to 1300 nm) with that obtained using methylene blue as a photo-sensitizer. Phosphorescence emission area, $Area_{phos,MB}$ is equal to the multiplication product between the absorbance of methylene blue at 650 nm (Ab_{MB-650}), incident light intensity at 650 nm (2 mW/cm^2, slit width: 10 nm) from the luminescence spectrometer, and the singlet O_2 formation yield (Φ_{MB}), i.e., the equation (1). The singlet O_2 quantum yield of MB in D_2O is known to be 0.68.

$$Area_{phos\text{-}MB} = Ab_{MB\text{-}650} \times I_{650} \times \Phi_{MB} \quad \ldots\ldots\ldots\ldots\ldots (1)$$

$$Area_{phos\text{-}MB} = 147338899$$

Similar equation can be derived for Au NPN 6.5(NaCl) (see equation (2))

$$Area_{phos\text{-}AuNPN6.5(NaCl)\text{-}1064\ nm} = Ab_{AuNPN6.5(NaCl)\text{-}1064\ nm} \times I_{1064} \times \Phi_{AuNPN6.5(NaCl)\text{-}1064\ nm} \quad \ldots\ldots\ldots\ldots\ldots(2)$$

$$Area_{phos\text{-}AuNPN6.5\ (NaCl)\text{-}1064nm} = 159633407$$

The incident light intensity of FLS 920 spectrometer at 1064 nm (~8.3 mW/cm^2, slit width: 10 nm). The absorbances of both methylene blue and Au NPN6.5(NaCl) solution at their excitation wavelengths were adjusted to 0.2. After substituting all the parameters and dividing equations (1)/ (2), one can obtain the value of $\Phi_{AuNPN6.5\ (NaCl)\text{-}1064\ nm}$ to be 0.354 @1064 nm.

Similarly, the singlet O_2 quantum yields of Au NPN6.5 (without filling $NaCl_{(aq)}$ in the nanogaps) at 1064 nm could be measured and calculated in the similar manner using the values of $Area_{phos\text{-}AuRS6.5\text{-}1064}$ = 82420167. The final singlet O_2 quantum yield for $\Phi_{AuNPN6.5\text{-}1064\ nm}$ was determined to be 0.183 @1064 nm.

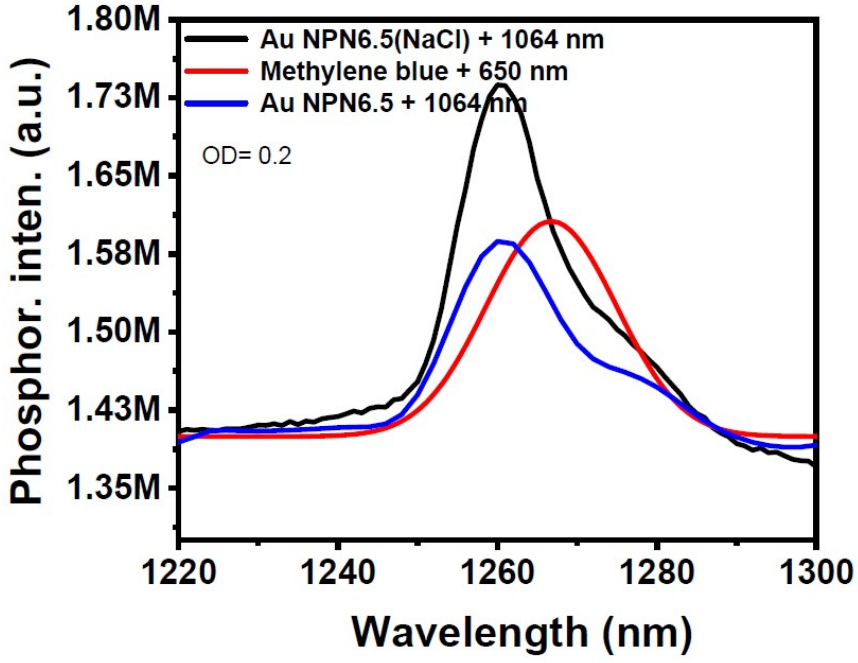

To calibrate the inner filter effects from (i.e., the absorption of singlet O_2 phosphorescence emission light by) Au NPNs on the singlet O_2 phosphorescence intensty detected within 1200-1300 nm range, the following equation for absorbance was used.

$$\text{Absorbance} = \log(I_0/I)$$

By substitutimg the absorbance of anti-h-EGFR-Au NPN6.5(NaCl) OD value 0.158 and anti-h-EGFR-Au NPN6.5 OD value 0.12 at 1260~1275 nm in the above equation yields 70% of light transmitted in case of anti-h-EGFR-Au NPN6.5(NaCl) and 76.3% of light transmitted in case of anti-h-EGFR-Au NPN6.5. Hence the final singlet O_2 qunamtum yields for $\Phi_{\text{AuNPN6.5 (NaCl)+1064 nm}}$ to be (0.354/0.7=) 0.51 @1064 nm and $\Phi_{\text{AuNPN6.5+1064 nm}}$ to be (0.183/0.763 =) 0.24 @1064 nm.

The singlet O_2 generation quantum yields are 0.24 and 0.51 for Au NPN6.5 and Au NPN6.5(NaCl) with OD= 0.2 at 1064 nm, respectively, which are slightly larger than those (0.20 and 0.42) for Au NPN6.5 samples with OD=0.1 at 1064 nm. The slightly larger singlet O2 quantum yields are most probably due to the more severe incident excitation ligtht scattering by Au NPNs. A more severe scattering of incident excitation light will increase the effective light path length and thus increased light absorption by the Au NPNs (ref. J. Phys. Chem. C 2018, 122, 27, 15625–15634). Therefore, the singlet O_2 quantum yields obtained from Au NPNs samples with OD= 0.1 is more reliable.

Calculation of fractions of PDT and PTT contributions in the photoinduced cellular deaths:

To determine the relative contribution of photodynamic and photothermal therapeutic effects on killing cancer cells, the cell incubation temperature was decreased from 37 to 4 ^{o}C to suppress the hyperthermia induced cellular deaths (i.e., suppress the photothermal effect). It must be noted that the ROS-mediated cellular deaths will not (or very slightly) be affected by lowering down the cell medium temperature, since chemical reactivity of ROS is not sensitive to small medium temperature variation from 37 to 4 ^{o}C). In a similar way, one can determine the relative contributions of NIR PDT- and PTT-induced cellular deaths for 1064 nm light irradiation.

The relative contributions of NIR PDT and NIR PTT of Au NPN6.5(NaCl) were calculated according to the literature reported procedures.[38-40] The therapeutic effect from 808 nm light irradiation was assumed to be 100% photothermal therapy (since there is no singlet oxygen was formed at this wavelength), whereas 1064 nm photo irradiation leads to combined NIR PDT and NIR PTT effects.

$$(d_1)_{\text{cell death,1064 nm,37 C}} = (\text{PDT})_{\text{1064 nm,37 C}} + (\text{PTT})_{\text{1064 nm,37 C}} \text{ ---------- (1)}$$

$$(d_2)_{\text{cell death,1064 nm,4 C}} = (\text{PDT})_{\text{1064 nm,4 C}} + (\text{PTT})_{\text{1064 nm,4 C}} \text{ ---------- (2)}$$

$$(d_3)_{\text{cell death,1064 nm,37 C}} = \text{PTT}_{\text{808 nm,37 C}} \text{ ---------- (3)}$$

$$(d_4)_{\text{cell death,1064 nm,4 C}} = \text{PTT}_{\text{808 nm,4 C}} \text{ ---------- (4)}$$

The values of d_1, d_2, d_3 and d_4 were determined experimentally. The ratio of d_4/d_3 was measured to be 0.65, i.e. by change in temperature of medium from 37 to 4 ^{o}C, photothermal induced cellular death was suppressed by 35% upon lowering down the cell medium

temperature from 37 to 4 °C. Likewise, the PTT-induced cellular death upon 1064 nm light irradiation is expected to be suppressed by 35% upon lowering down the cell medium temperature from from 37 to 4 °C.

$$PTT_{808\ nm,4\ C}/PTT_{808\ nm,37\ C} = d_4/d_3 = 0.65 \text{ ---------- (5)}$$

Substituting eq. (5) into the eq. (2) results in

$$d_2 = (PDT)_{1064\ nm,\ 4\ C} + [d_4/d_3]\ (PTT)_{1064\ nm,\ 37\ C} \text{---------- (6)}$$

Let a = $(PDT)_{1064\ nm,\ 37\ C}$ and b = $(PTT)_{1064\ nm,\ 37\ C}$

Let us assume negligible or minor effect of temperature on PDT cell death, we get $(PDT)_{1064\ nm,4\ C} = a = (PDT)_{1064\ nm,37\ C}$. Then eq. (1) and (2) can be re-write as

$$d_1 = a + b \text{ ---------- (1x)}$$

$$d_2 = a + 0.65\ b \text{ ---------- (1y)}$$

By substituting the d_1, d_2, d_3, and d_4 experimental values and solving the eq. (1x) and (1y), one can get the value of a and b, i.e. $(PDT)_{1064\ nm,37\ C}$ and $(PTT)_{1064\ nm,37\ C}$. Finally, for each concentration of Au NPN6.5(NaCl) the values of corresponding $(PDT)_{1064nm,37\ C}$, $(PDT)_{1064\ nm,4\ C}$, $(PTT)_{1064\ nm,37\ C}$, and $(PTT)_{1064\ nm,4\ C}$.

The similar calculations were carried out for the 1064 nm laser irradiations to determine the relative contributions of PDT and PTT in the Au NPN6.5 system. The values of d_1, d_2, d_3 and d_4 were determined experimentally. The ratio d_4/d_3 is obtained as 0.45, i.e. by change in temperature of medium from 37 to 4 °C, photothermal induced cellular death was suppressed by 55 %.

By substituting the d_1, d_2, d_3, and d_4 experimental values and solving the eq. (1x) and (1y), one can get the value of a and b, i.e. $(PDT)_{1064\ nm,37\ C}$ and $(PTT)_{1064\ nm,37\ C}$. Finally, for each concentration of Au NPN6.5 the values of corresponding $(PDT)_{1064\ nm,37\ C}$, $(PDT)_{1064\ nm,4\ C}$, $(PTT)_{1064\ nm,37\ C}$, $(PTT)_{1064\ nm,4\ C}$.

For the evaluation of contribution of Au NPN6.5(NaCl) for NIR PDT and NIR PTT, CT-26 cancer cells were incubated with Au NPN6.5(NaCl) at 37 °C. From the singlet O_2 phosphorescence emission spectra (Figure 2(d) in the main text), it is clearly understood that at 808 nm laser irradiation, hyperthermia is responsible for all the cellular deaths. The percentage of PDT and PTT effects at 1064 nm laser exposure (at 37 °C) are 57 % PDT + 14.5 % PTT in a total of 71.5% cell deaths at a dose of 50 μg/mL of Au NPN6.5(NaCl). The fractions of PDT and PTT effects at 1064 nm laser exposure (at 37 °C) are 30 % PDT + 11 % PTT in a total of 41 % cell deaths at 50 μg/mL of Au NPN6.5.

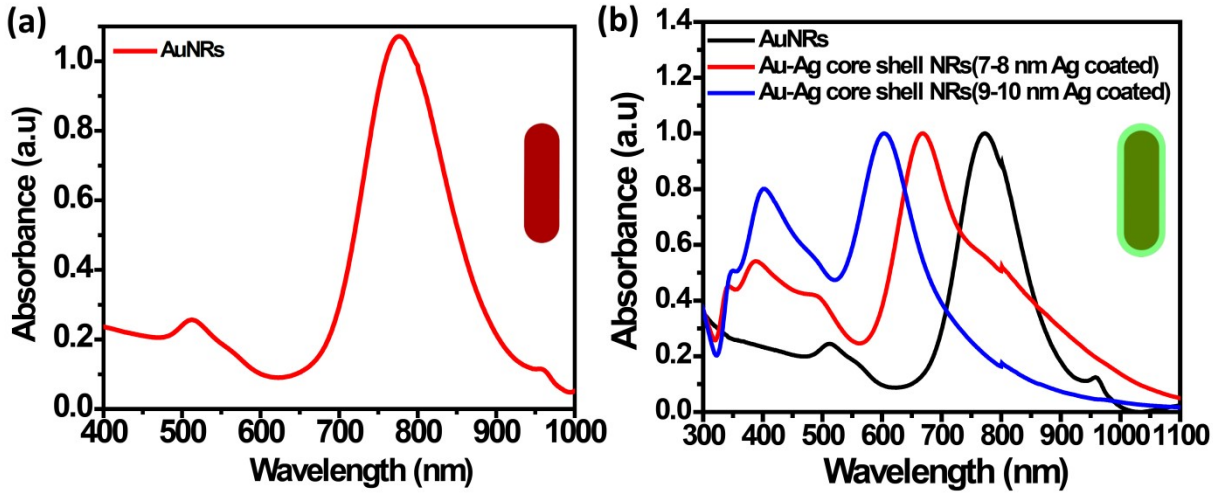

Figure S1. Characterization of optical properties. Uv-vis-NIR spectrum for (a) as-synthesized Au NRs (aspect ratio 4.0); (b) as-synthesized Au NR@Ag core-shell NRs with different thickness of Ag shell over Au NRs.

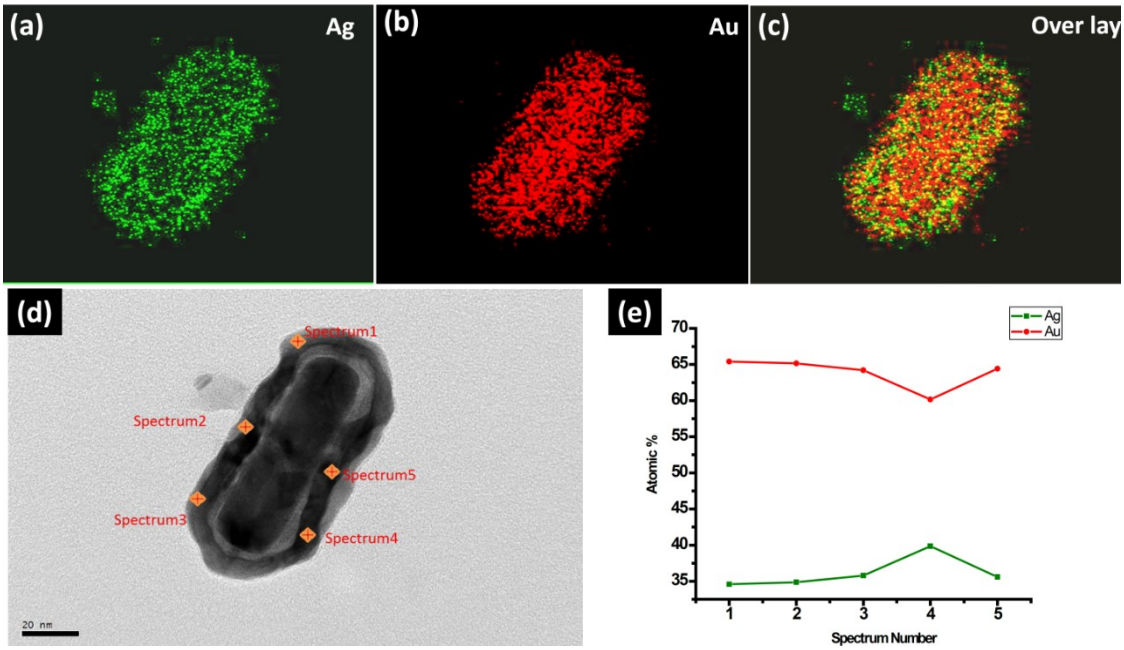

Figure S2 EDAX and TEM images of as-synthesized Au NPN6.5. Elemental mapping images of (a) Ag; (b) Au; (c) overlay of Au NPN6.5; (d) TEM image of Au NPN6.5 representing the mapping spectral points of EDAX recorded. (e) Atomic % of Au and Ag in the Au NPN6.5 measured at different spectral points.

Table S1. Molar extinction coefficients of organic dyes, nanomaterials and the as-synthesized Au NPN2.0(NaCl) and Au NPN6.5(NaCl).

S.No.	Photoabsorber	Size (nm)	Wavelength (nm)	Molar extinction coefficient ($M^{-1}cm^{-1}$)
1.	Rhodamine 6G	Molecular	530	1.2×10^5
2.	Malachite Green	Molecular	530	1.5×10^5
3.	PEG-$W_{18}O_{49}$ nanowires	1 nm	980	0.5×10^7
4.	Copper sulfide nanocrystal	7 nm	808	9.5×10^8
5.	Copper selenide	16 nm	980	7.7×10^7
6.	AuNEs	350 nm	915	0.69×10^{12}
7.	AuNEs	350 nm	1064	0.74×10^{12}
8.	AuNPN 2.0 (NaCl)	86 nm	1064	0.96×10^{11}
9.	AuNPN 6.5(NaCl)	92 nm	1064	1.95×10^{11}

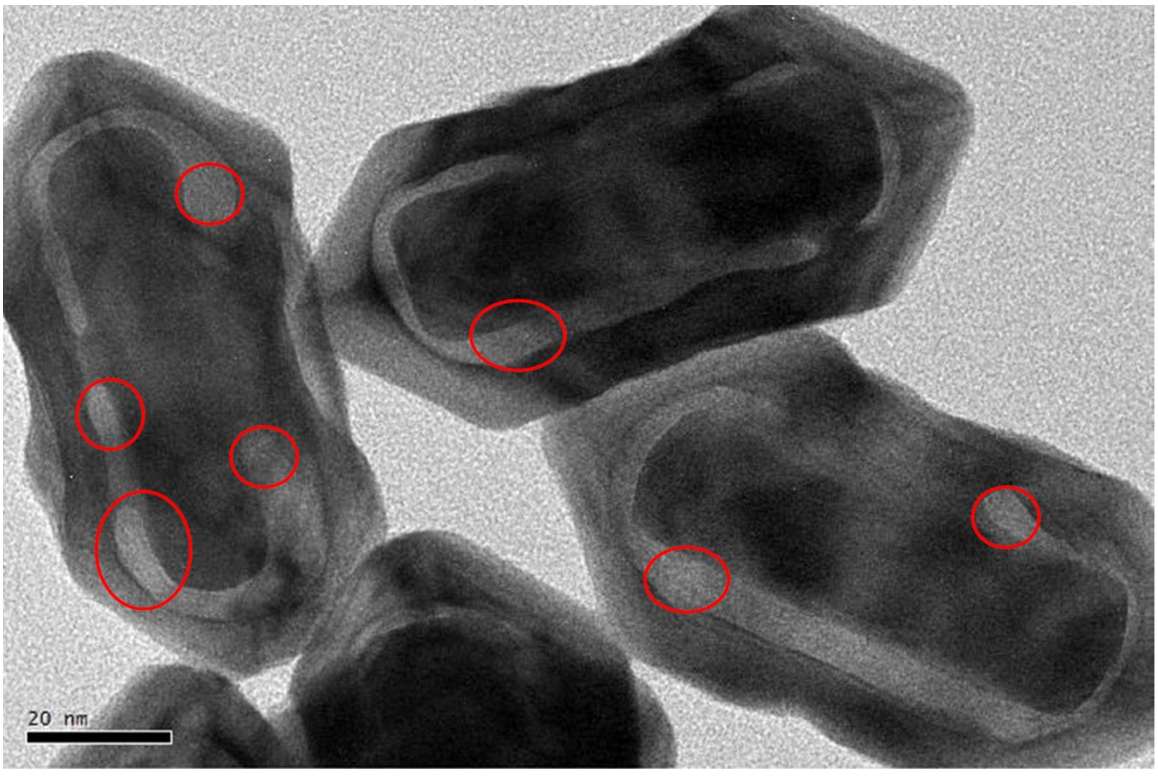

Figure S3. TEM images of as-synthesized Au NPN6.5 with nanopores on the outer shells of the nanostructures (marked area by red circles).

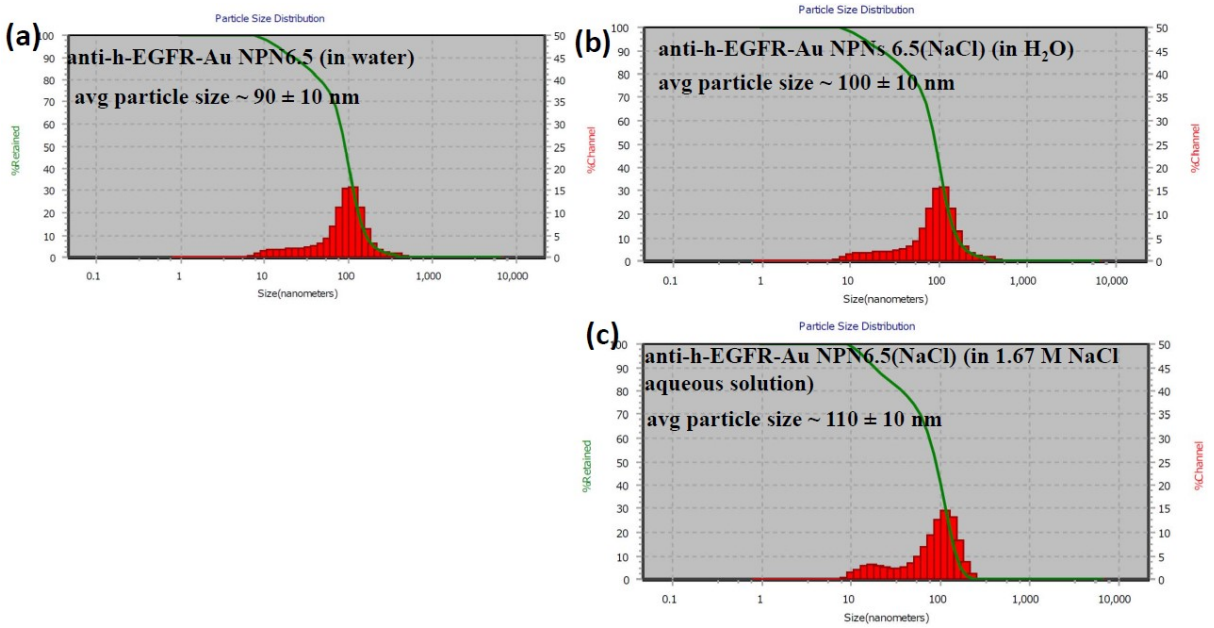

Figure S4. DLS particle size measurements of anti-h-EGFR-Au NPN6.5 in pure water (a) before and (b) after filling $NaCl_{(aq)}$ into the nanogaps. (c) DLS particle size measurements of anti-h-EGFR-Au NPN6.5(NaCl) in 1.67 M NaCl aqueous solution. To avoid any salt induced aggregation problem, low concentrations (OD= 0.1 at 1064 nm) of Au NPN6.5 and Au NPN6.5(NaCl) in aqueous solution (no salt) were used in the DLS measurements. Note that the x-axis is in a $\log_{10}$ scale, not a linear scale. The first minor tick at the middle point between 100 and 1000 is corresponding to an average particle size of 316 nm ($\log_{10}$ x= 2.5, then x= $10^{2.5}$= 316 nm).

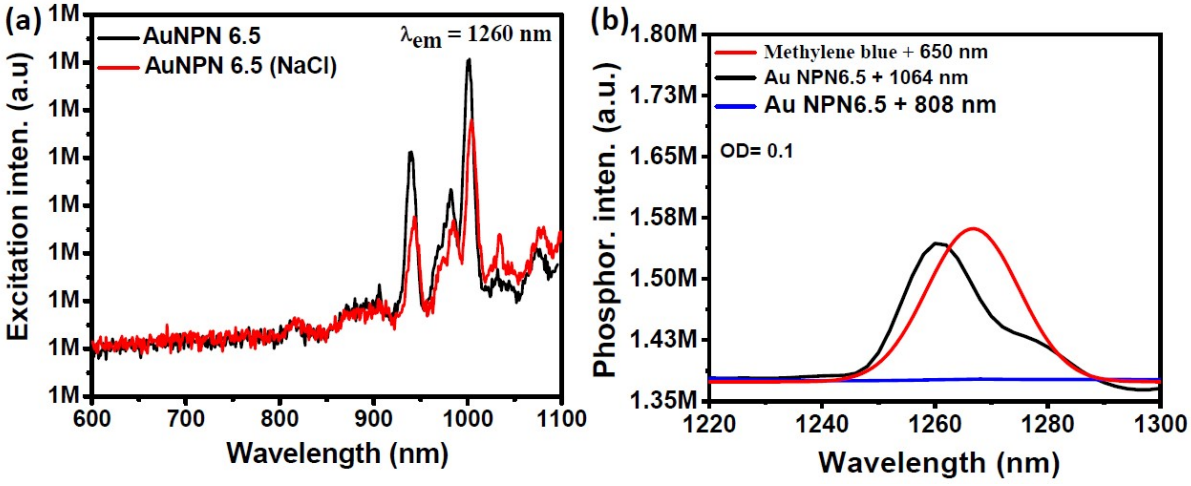

Figure S5. Singlet oxygen excitation spectra and phosphorescence emission spectra. (a) Singlet oxygen excitation profiles of Au NPN6.5 and Au NPN6.5(NaCl) with emission wavelength set at 1260 nm. (b) Singlet O_2 emission spectra from Au NPN6.5 (without filling $NaCl_{(aq)}$ in the nanogaps) under different excitation wavelengths λ_{ex} at 808 and 1064 nm, respectively, as indicated in the spectra. The singlet oxygen phosphorescence emission spectra were recorded from an Au NPN6.5 aqueous solution with OD= 0.1 at 1064 nm. When the OD at 1064 nm is too high, for example OD= 0.5 at 1064 nm, the singlet O_2 phosphorescence emission spectrum will be distorted due to the inner filter effect, i.e., the absorption of singlet O_2 emission light by Au NPN6.5.

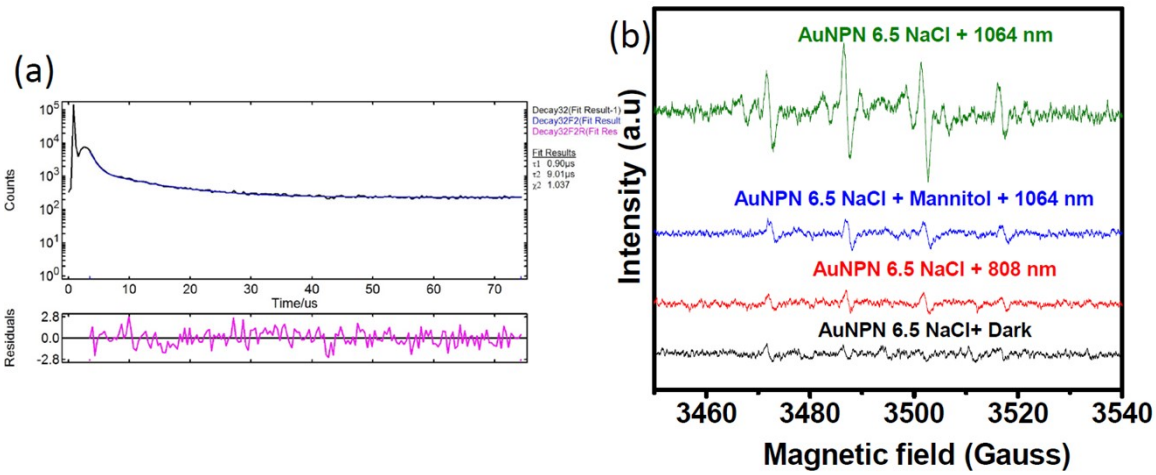

Figure S6. Singlet oxygen lifetime and hydroxyl radical EPR spectra measurements. (a) Singlet O_2 lifetime measurements from Au NPN6.5(NaCl) under excitation wavelength λ_{ex}= 1064 nm and emission wavelength set at 1260 nm. (b) EPR measurements for detection of hydroxyl radicals generated from anti-EGFR-AuNPN6.5(NaCl) nanostructures upon NIR light (808 or 1064 nm) irradiation.

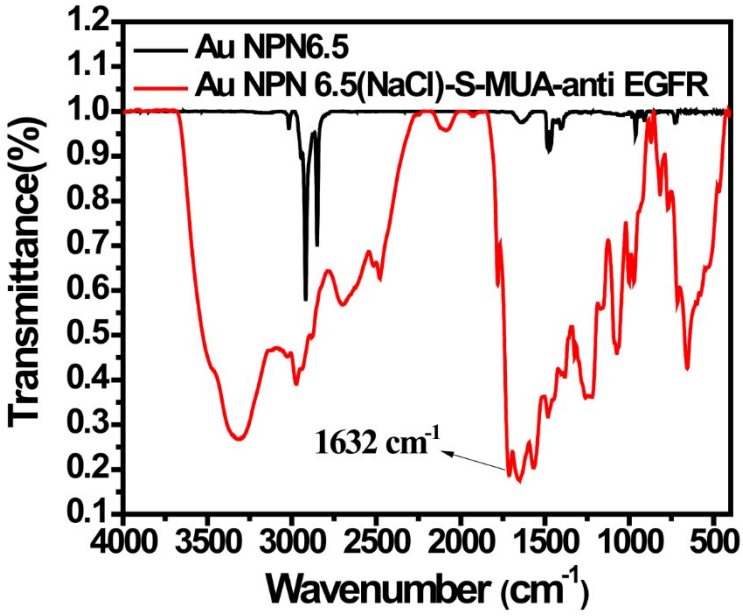

Figure S7. FT-IR spectra for Au NPN6.5 and functionalized Au NPN6.5(NaCl)-S-MUA-anti-h-EGFR.

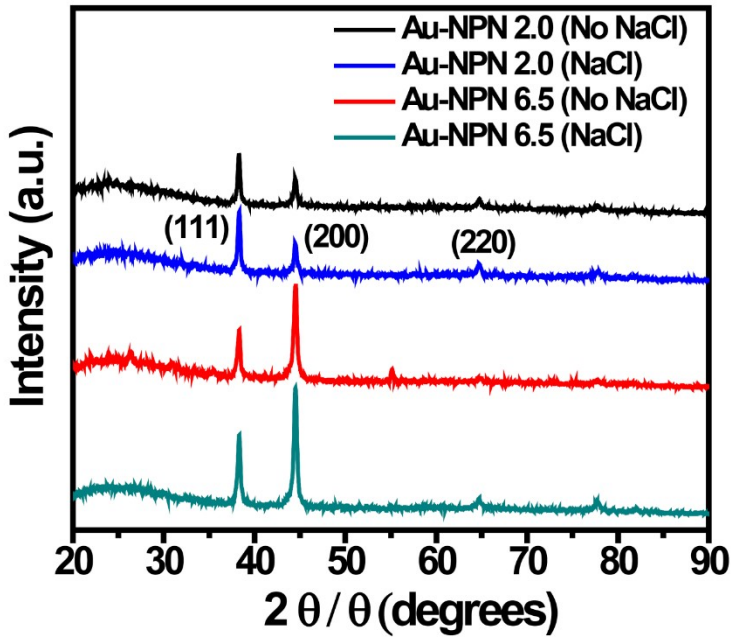

Figure S8. X-ray diffraction analysis of Au NPN with conditions 2.0, 6.5, 2.0 (NaCl) and 6.5 (NaCl)

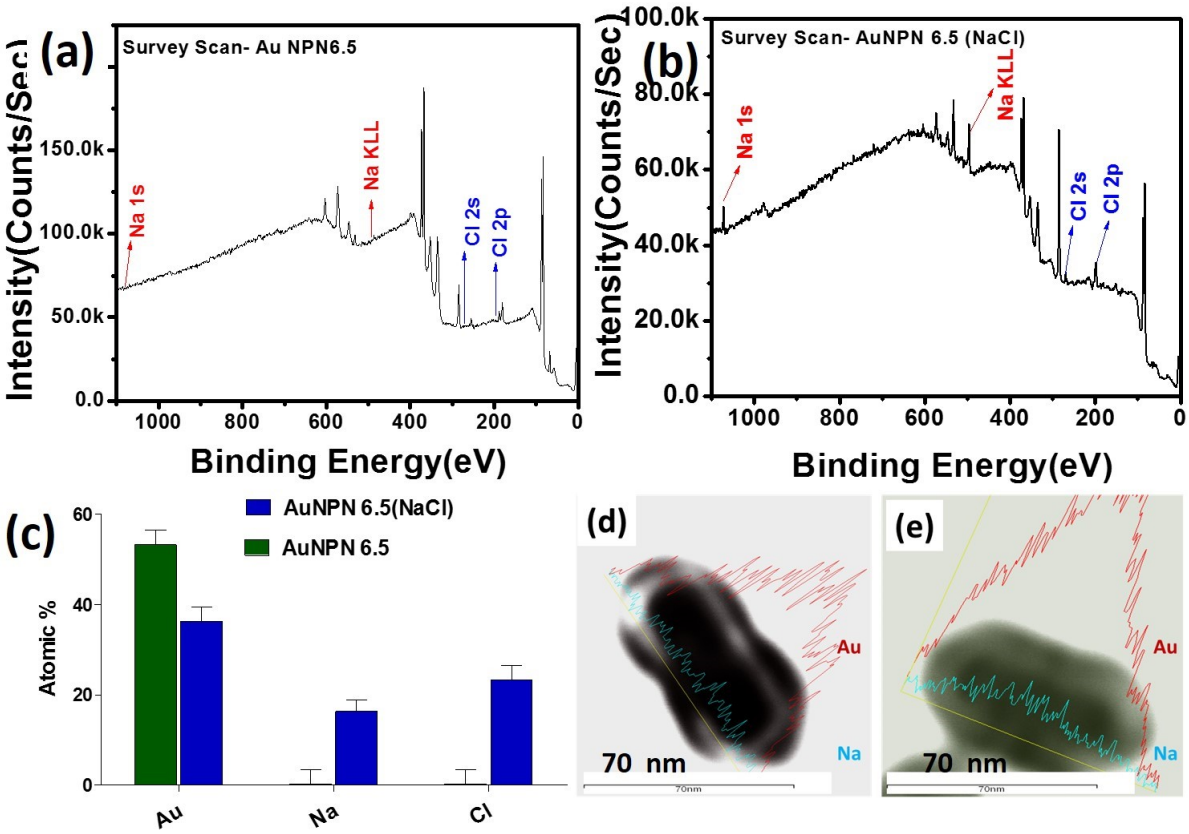

Figure S9. XPS measurements of (a) Au NPN6.5, and (b) Au NPN6.5(NaCl)(1.67M). (c) Atomic percentages of Au, Na, and Cl elements obtained from the XPS data shown in (a) and (b). The AuNPN6.5(NaCl) sample was prepared by soaking AuNPN6.5 in an aqueous solution containing 1.67 M NaCl for overnight, following by centrifugation to collect the AuNPN6.5(NaCl) ppt. The collected AuNPN6.5(NaCl) precipitate was rinsed with DI water to remove residual NaCl on the outside of nanoparticles before XPS analysis. TEM-EDX line scan mapping intensities of the Au and Na elements, respectively, in (d) AuNPN6.5, and (e) AuNPNs6.5(NaCl) nanostructures. The intensities of Au and Na elements were plotted in the figures. The scale bar is 70 nm.

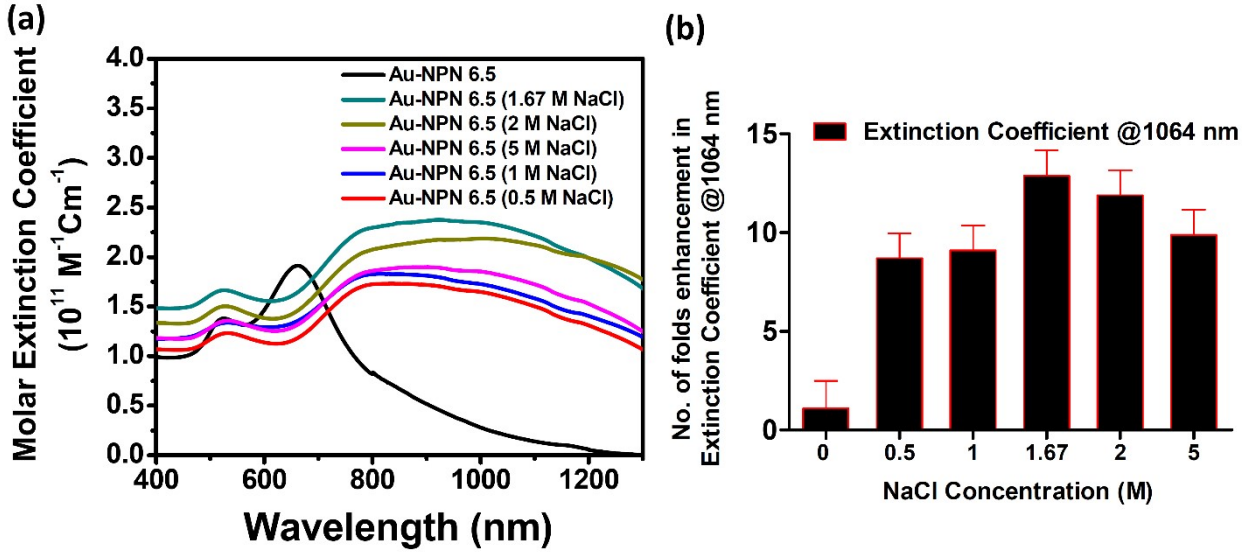

Figure S10. Tuning optical properties by filling $NaCl_{(aq)}$ into the nanogaps of Au NPN6.5. (a) Molar extinction coefficient for Au NPNs6.5 with different NaCl concentrations ranging from 0, 0.5, 1, 1.67, 2, and 5 M, respectively. (b) Effect of $NaCl_{(aq)}$ in the nanogaps on molar extinction coefficient at 1064 nm, expressed in terms of fold for Au NPNs6.5(NaCl) with NaCl concentration ranging from 0, 0.5, 1, 1.67, 2, and 5 M, respectively.

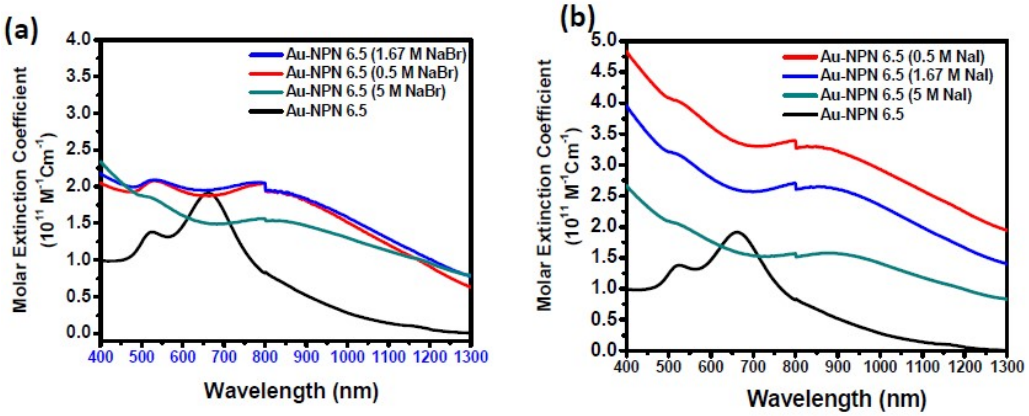

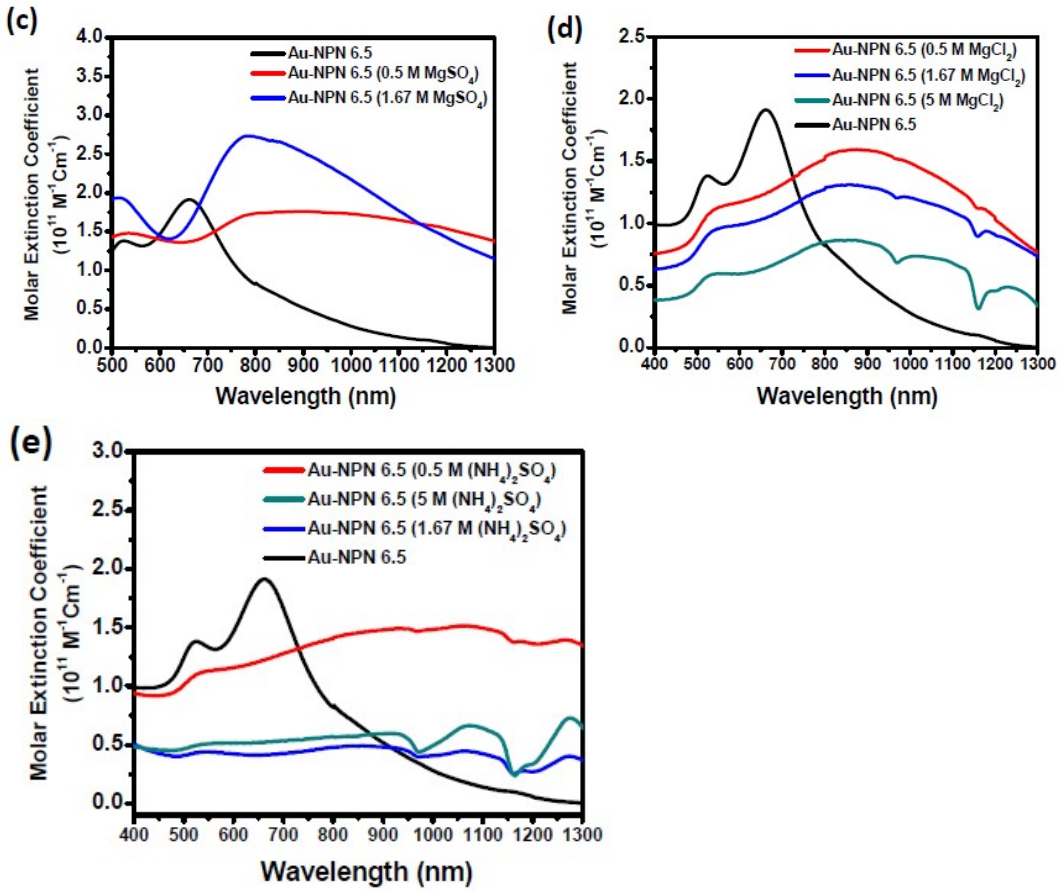

Figure S11. Molar extinction coefficients of Au NPNs6.5salt with filling of different highly dielectric salts into the nanogaps: (a) NaBr, (b) NaI, (c) $MgSO_4$ (d) $MgCl_2$ (e) $(NH_4)_2SO_4$

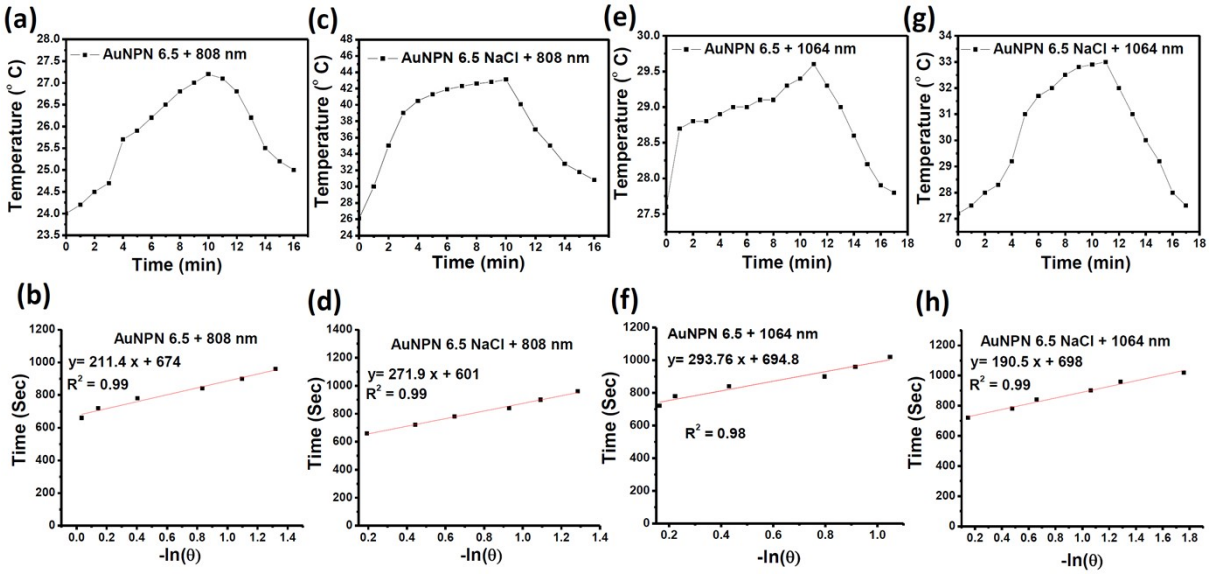

Figure S12. Photothermal conversion efficiencies (η) for both Au NPN6.5, and Au NPN6.5(NaCl) at 808 nm and 1064 nm laser excitation wavelengths, respectively. (a), (c), (e), and (g) represent the photothermal temperature elevation profiles of Au NPN6.5 and Au NPN6.5(NaCl) aqueous solutions at 808 nm (200 mW/cm^2; 10 min) and 1064 nm (200 mW/cm^2; 11 min). (b), (d), (f), and (h) represent laser irradiation time vs. –ln(Θ) plots, which were calculated from the cooling profiles of (a), (c), (e), and (g), respectively.

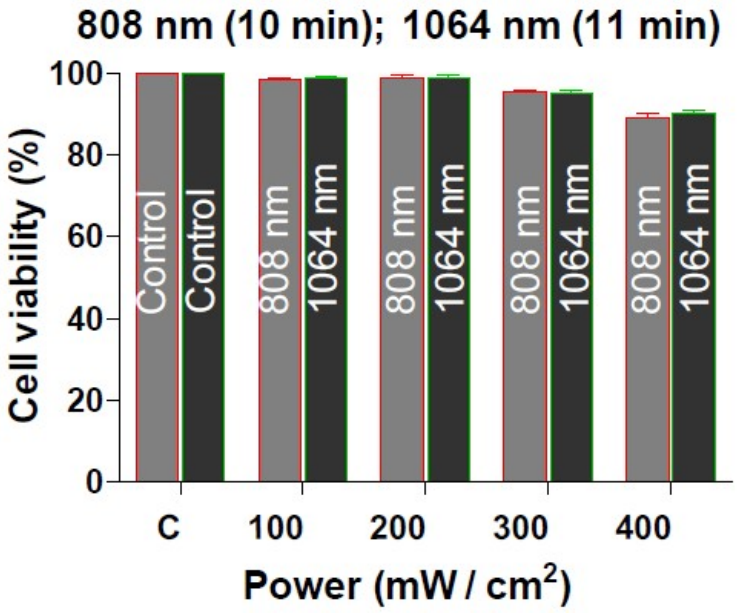

Figure S13. Cell viabilities of a control group as a function of laser irradiation power at 808 nm (200 mW/cm^2, 10 min) and 1064 nm (200 mW/cm^2, 11 min), respectively.

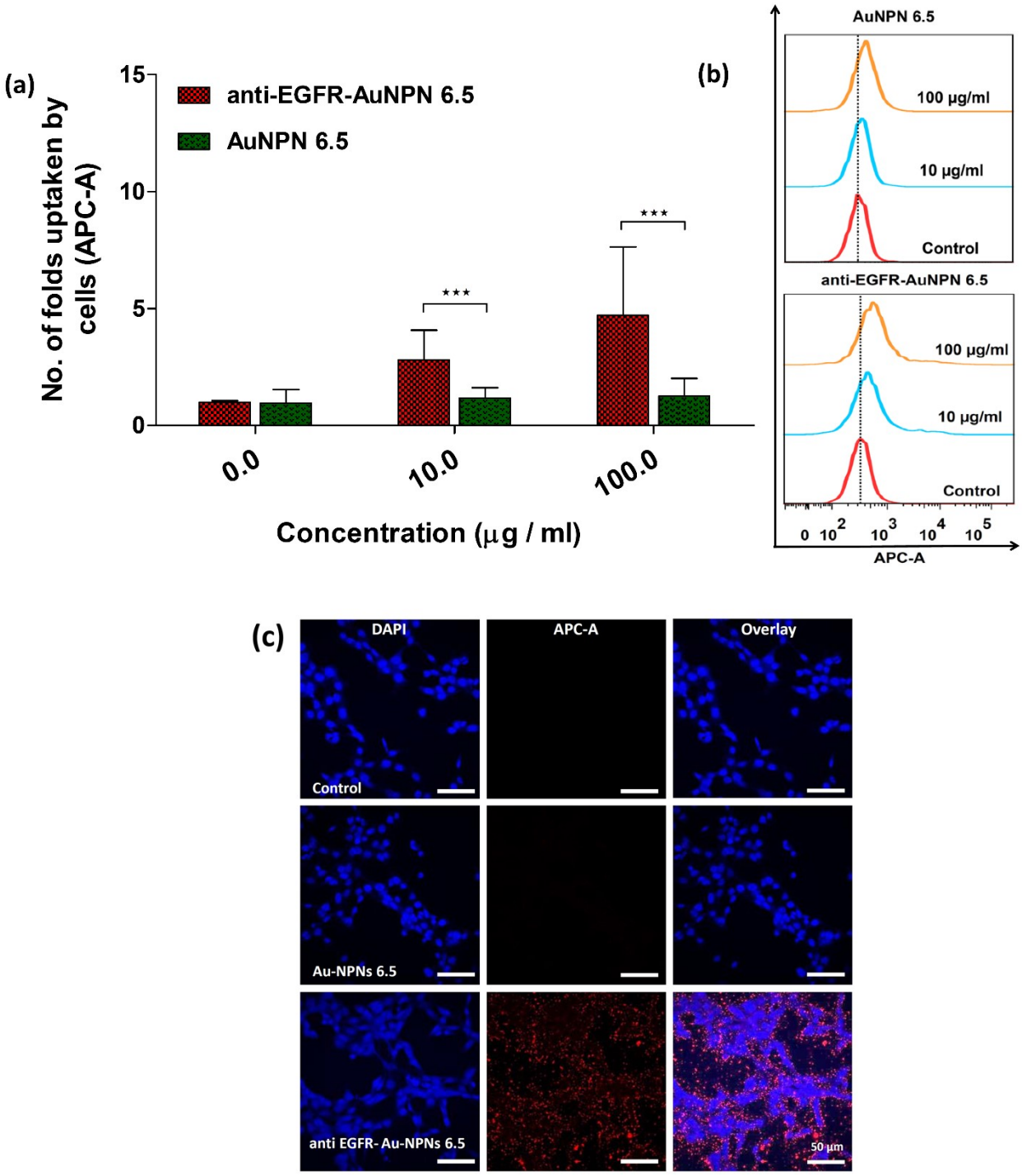

Figure S14. Targeting ability of anti-EGFR-Au NPNs6.5(NaCl). (a)~(b) The mean fluorescence intensities of CT-26 cells treated with Au NPNs6.5(NaCl) (without anti-EGFR), and anti-EGFR-Au NPNs6.5(NaCl), respectively, monitored by flow cytometry. (c) Confocal images of CT-26 cells treated with PBS, Au NPNs6.5(NaCl) and anti-EGFR-Au NPNs6.5(NaCl), respectively, followed by pretreatment using Cy5®goat anti-mouse IgG secondary antibody. The scale bar is 50 μm.

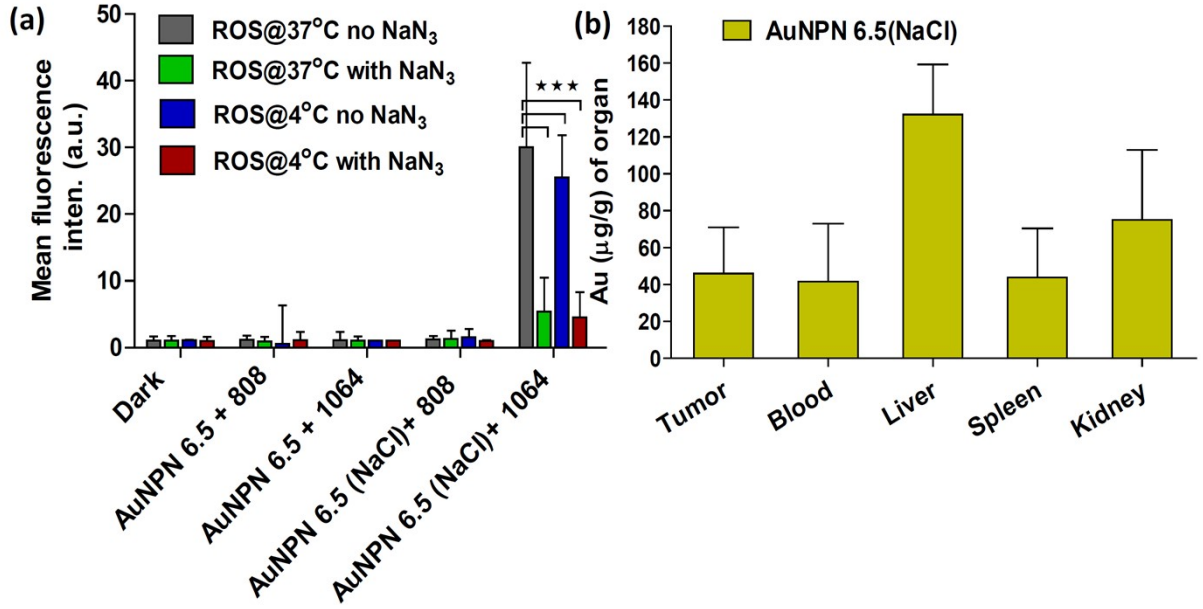

Figure S15. In vitro ROS detection in cells, and in vivo targeting analysis. (a) ROS generation from CT26 colon cancers fed with Au NPN6.5, and Au NPN6.5(NaCl), respectively, under photo irradiation of different wavelengths at 4 and 37 °C. The ROS level was measured using ROS-specific fluorescence probe, DCFH-DA. (b) Bio-distribution of Au NPN6.5, Au NPN6.5(NaCl) in major organs. Major organs were collected at 24 h after i.v. injection of nanomaterials, and analyzed by ICP-MS.

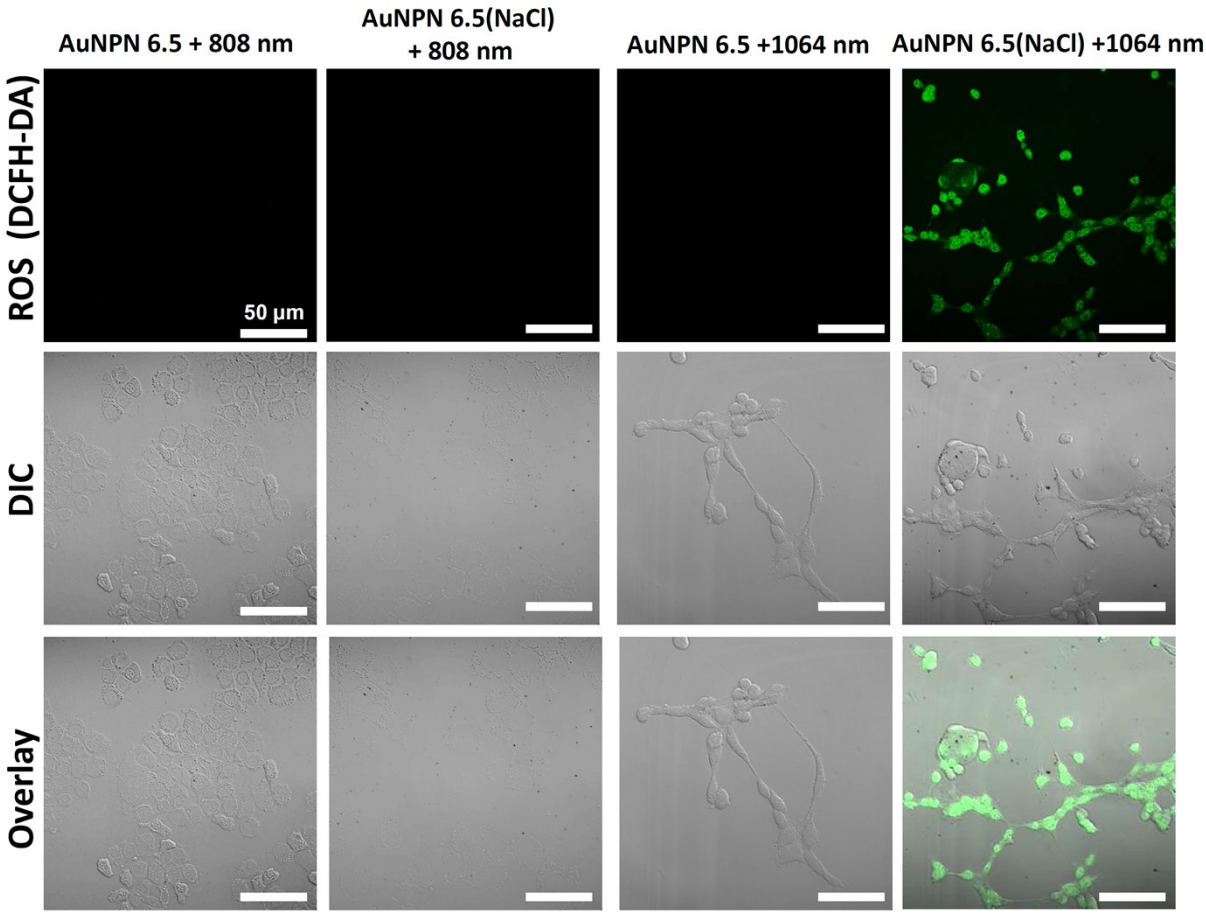

Figure S16. ROS detection through in vitro confocal optical imaging with the probe DCFH-DA and laser irradiations of Au NPN6.5 and Au NPNs6.5(NaCl) by 808 (200 mW/cm^2, 10 min) and 1064 nm (200 mW/cm^2, 11 min), respectively.

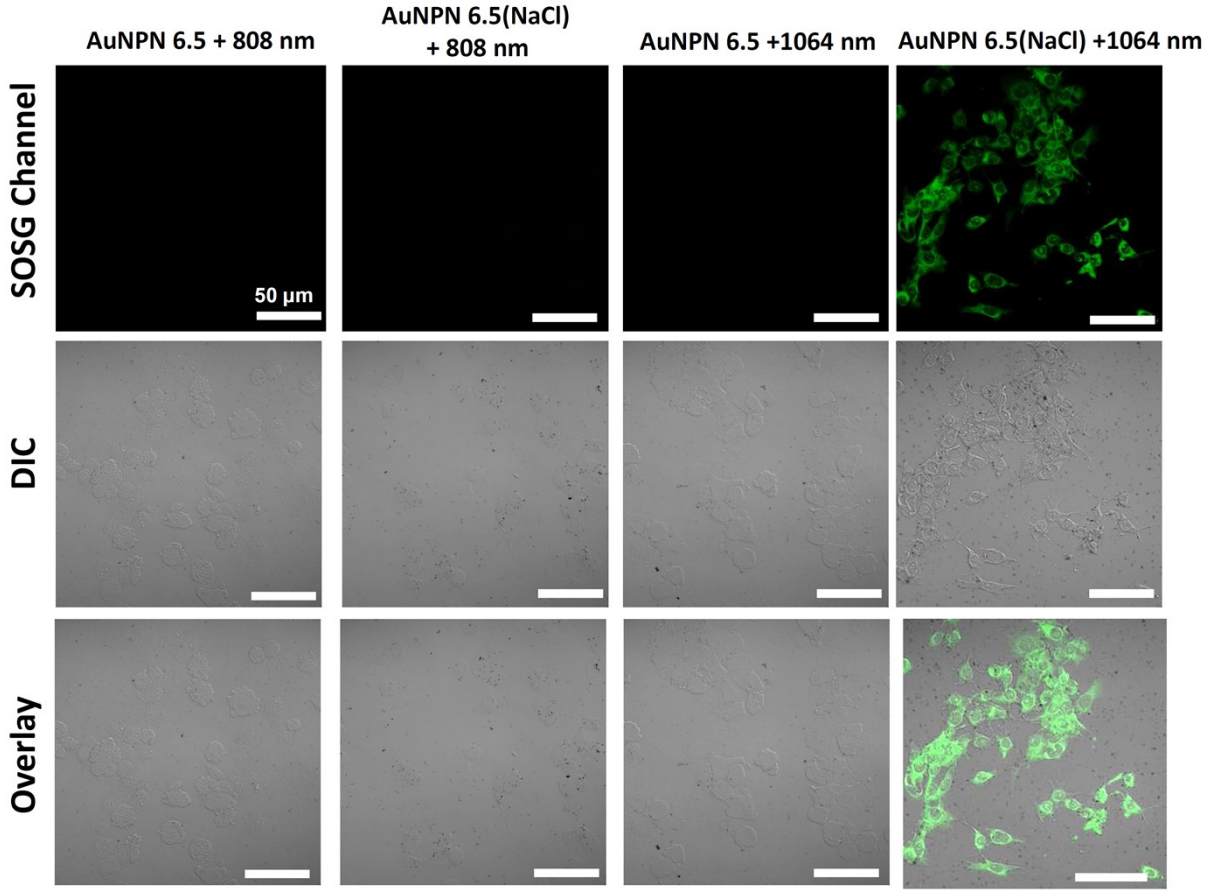

Figure S17. Singlet oxygen detection through in vitro confocal optical imaging using singlet oxygen-specific probe SOSG via 808 and 1064 nm laser excitation of Au NPN6.5 and Au NPN6.5(NaCl), respectively.

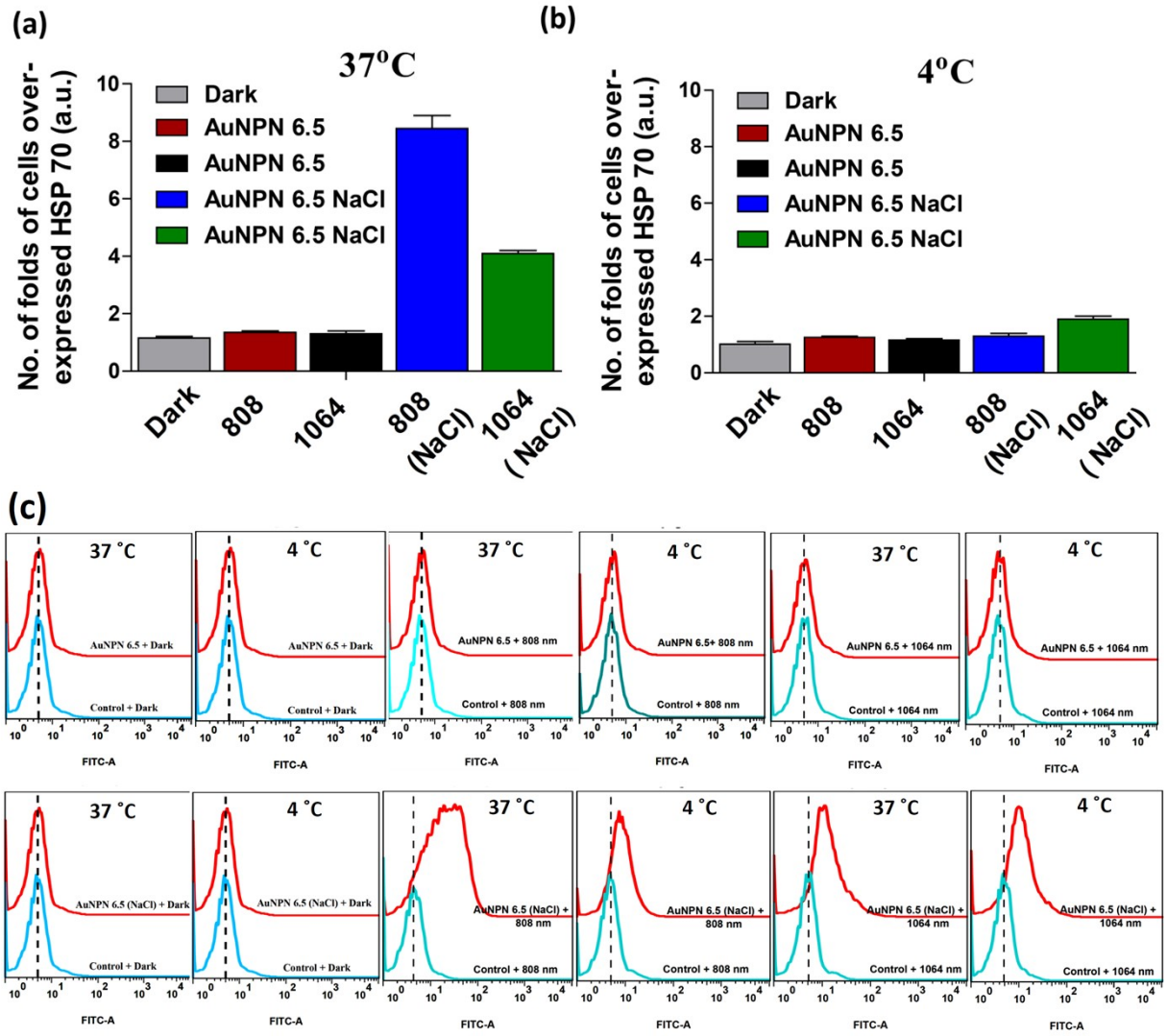

Figure S18. In vitro heat shock protein HSP-70 expression. The expression levels of HSP-70 were measured from CT-26 colon cancer cells treated with Au NPN6.5, and Au NPN6.5(NaCl), respectively, at (a) 37 °C and (b) 4 °C under different laser irradiation conditions as indicated in the figure. (c) Flow cytometry histograms for the heat shock protein HSP-70 expression (measured in the FITC channel) for different groups as labeled in the figures.

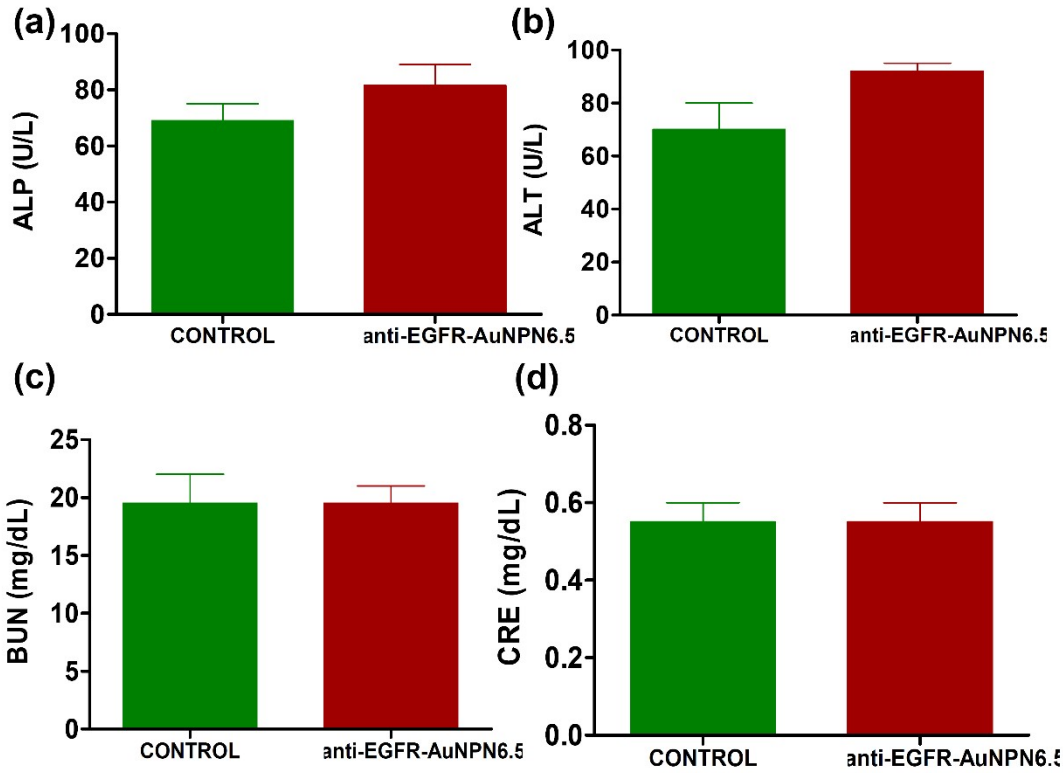

Figure S19. Hematology analysis for the nephritic and hepatic functions of BALB/C nude mice at day 45th post i.v. injection of anti-EGFR-Au NPNs6.5(NaCl) at a 50 mg/kg dosage. (a)~(b) Hepatic function of liver with alkaline phosphatase (ALP), aminotransferase (ALT) levels. (c)~(d) Nephritic function of kidneys with blood urea nitrogen (BUN) and creatinine (CR) levels.

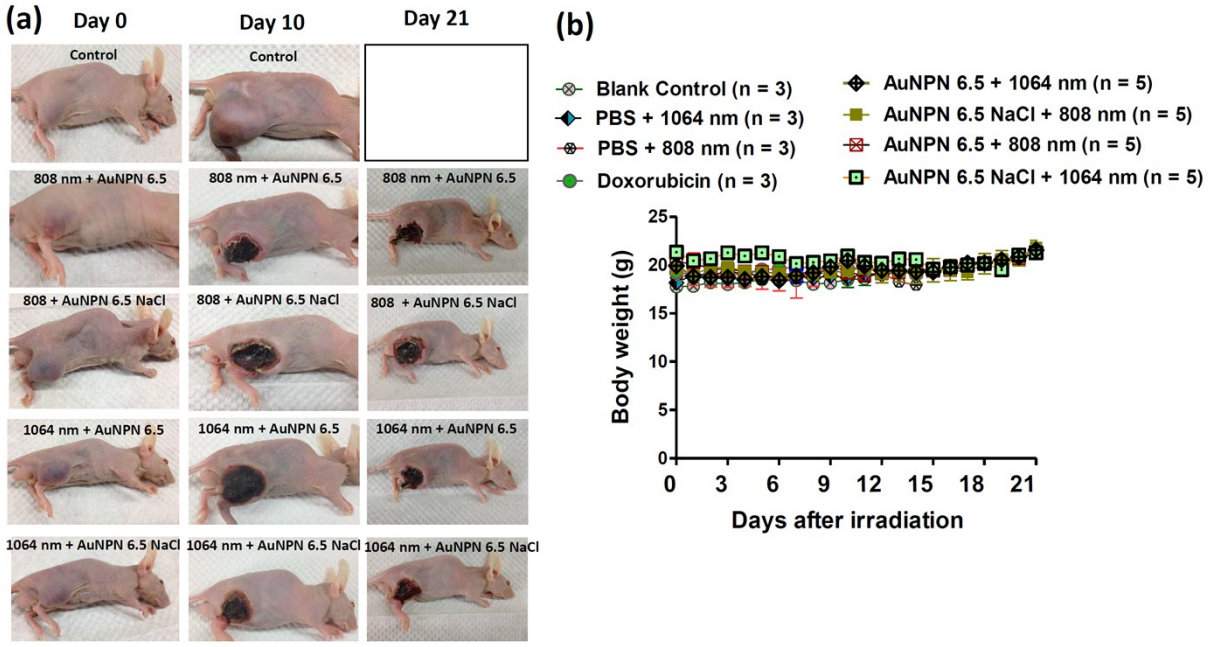

Figure S20. In vivo therapeutic results showing (a) the images of the tumor sites at different days during the therapy period, and (b) the body weight curves monitored for the mice during the therapy period.

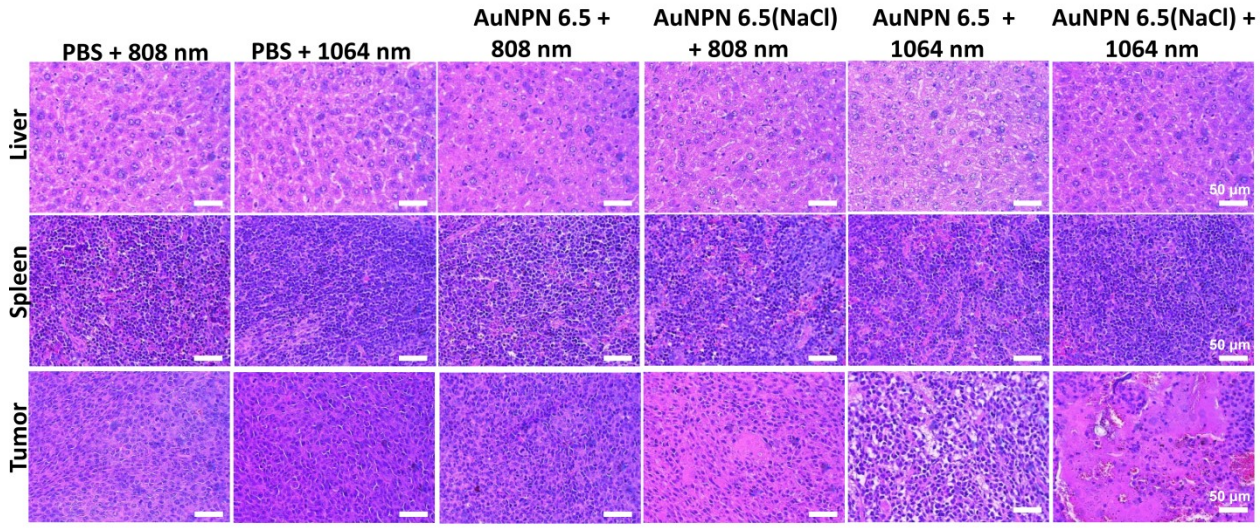

Figure S21. Evaluation of therapeutic effects on damages to major organs, including liver, spleen and tumor via Haemotoxilin and Eosin (H&E) staining.